Inorg. Chem. **2003**, *42*, 6306–6313

Photochemical Behavior of Azobenzene-Conjugated Co^{II}, Co^{III}, and Fe^{II} Bis(terpyridine) Complexes

Tomona Yutaka,[†] Ichiro Mori,[†] Masato Kurihara,[†] Naoto Tamai,[‡] and Hiroshi Nishihara*[,†]

Department of Chemistry, School of Science, The University of Tokyo, 7-3-1 Hongo, Bunkyo-ku, Tokyo 113-0033, Japan, and Department of Chemistry, Faculty of Science, Kwansei Gakuin University, 1-1-155 Uegahara, Nishinomiya, Hyogo 662-8501, Japan

Received September 19, 2002

Azobenzene-conjugated mononuclear and dinuclear terpyridyl complexes of Co^{II}, Co^{III}, and Fe^{II} were synthesized, and their photoisomerization behavior was investigated. Co^{II} and Co^{III} complexes, $[tpyCo(tpy\text{-}AB)]X_n$ and $[(Cotpy)_2(tpy\text{-}AB\text{-}tpy)]X_n$ (tpy-AB = $C_{15}N_3H_{10}$—C_6H_4—N=NC_6H_5, tpy-AB-tpy = $C_{15}N_3H_{10}$—C_6H_4—N=NC_6H_4—$C_{15}N_3H_{10}$, X = PF_6 or BPh_4), exhibit trans-to-cis photoisomerization by irradiation at 366 nm, and this behavior is dependent on solvents and counterions. For the Co^{II} complexes, BPh_4 salts undergo cis-to-trans isomerization in propylene carbonate by both photoirradiation with visible light (435 nm) and heat, indicating that reversible trans–cis isomerization has occurred. $[Co(tpy\text{-}AB)_2](BPh_4)_2$ shows a two-step trans-to-cis isomerization process. The trans–cis isomerization behavior of Co^{III} complexes was observed only in the solvents with a low donor number such as 1,2-dichloroethane. Fe^{II} complexes, $[tpyFe(tpy\text{-}AB)]X_n$ (X = PF_6 or BPh_4), exhibit slight trans-to-cis photoisomerization due to the energy transfer from the azobenzene moiety to $Fe(tpy)_2$ moieties.

Introduction

Azobenzene[1] and its derivatives undergo reversible trans−cis isomerization in response to photo and thermal input, and much effort has been devoted to clarifying the isomerization mechanism.[2] Moreover, such isomerization of azobenzenes is the current subject of research interest in the area of photon-mode high-density information storage and photoswitching devices.[3] Recently, metal complexes including azobenzene and related compounds as building blocks have been synthesized,[4] and a number of studies concerned with the photoisomerization of azo-conjugated metal complexes have been reported.[5,6] This recent activity is due to the potential for azo-conjugated transition metal complexes to provide new advanced molecular functions based on combinations of photoisomerization of the azo group and changes in the intrinsic properties, i.e., in the optical, redox, and magnetic properties originating from the d-electrons. Some of the reported complexes have actually shown novel behavior not generally observed for organic azobenzenes, including reversible isomerization by the combination of the

* To whom correspondence should be addressed. E-mail: nisihara@chem.s.u-tokyo.ac.jp. Fax: +81-3-5841-8063. Phone: +81-3-5841-4346.
[†] University of Tokyo.
[‡] Kwansei Gakuin University.

(1) (a) Hartley, G. S. *Nature* **1937**, *140*, 281. (b) Hartley, G. S. *J. Chem. Soc.* **1938**, 633−642. (c) Hartley, G. S.; Le Fevre *J. Chem. Soc.* **1939**, 531−535.
(2) (a) Sekkat, Z.; Wood, J.; Knoll, W. *J. Phys. Chem.* **1995**, *99*, 17226−17234. (b) Cimiraglia, R.; Asano, T.; Hofmann, H.-J. *Gazz. Chim. Ital.* **1996**, *126*, 679−684. (c) Sanchez, A. M.; de Rossi, R. H. *J. Org. Chem.* **1996**, *61*, 3446−3451. (d) Lednev, I. K.; Ye, T.-Q.; Hester, R. E.; Moore, J. N. *J. Phys. Chem.* **1996**, *100*, 13338−13341. (e) Cattaneo, P.; Persico, M. *Phys. Chem. Chem. Phys.* **1999**, *1*, 4739−4743. (f) Sanchez, A. M.; Barra, M.; de Rossi, R. H. *J. Org. Chem.* **1999**, *64*, 1604−1609. (g) Tamai, N.; Miyasaka, H. *Chem. Rev.* **2000**, *100*, 1875−1890. (h) Fujino, T.; Tahara, T. *J. Phys. Chem.* **2000**, *A104*, 4203−4210.
(3) (a) Rau, H. *Photochromism. Molecules and Systems*; Dürr, H. B., Laurent, H., Eds; Elsevier: Amsterdam, 1990; p 165. (b) Junge, D. M.; McGrath, D. V. *J. Chem. Soc., Chem. Commun.* **1997**, 857−858. (c) Röttger, D.; Rau, H. *J. Photochem. Photobiol.* **1999**, *A101*, 205−214. (d) Yamaguchi, T.; Nakazumi, H.; Irie, M. *Bull. Chem. Soc. Jpn.* **1999**, *72*, 1623−1627. (e) Feringa, B. L.; von Delden, R. A.; Koumura, N.; Geertsema, E. M. *Chem. Rev.* **2000**, *100*, 1789−1816.
(4) (a) Launay, J.-P.; Tourrel-Paagis, M.; Libskier, J.-F.; Marvaud, V.; Joachim, C. *Inorg. Chem.* **1991**, *30*, 1033−1038. (b) Das, A.; Maher, J. P.; McCleverty, J. A.; Badiola, J. A. N.; Ward, M. D. *J. Chem. Soc., Dalton Trans.* **1993**, 681−686. (c) Otsuki, J.; Sato, K.; Tsujino, M.; Okuda, N.; Araki, K.; Seno, M. *Chem. Lett.* **1996**, 847−848. (d) Otsuki, J.; Tsujino, M.; Iizaki, T.; Araki, K.; Seno, M.; Takatera, K.; Watanabe, T. *J. Am. Chem. Soc.* **1997**, *119*, 7895−7896. (e) Kurihara, M.; Kurosawa, M.; Matsuda, T.; Nishihara, H. *Synth. Met.* **1999**, *102*, 1517−1518. (f) Kurosawa, M.; Nankawa, T.; Matsuda. T.; Kubo, K.; Kurihara, M.; Nishihara, H. *Inorg. Chem.* **1999**, *38*, 5113−5123. (g) Noro, S.; Kondo, M.; Ishii, T.; Kitagawa, S.; Matsuzaka, H. *J. Chem. Soc., Dalton Trans.* **1999**, 1569−1574. (h) Sun, S.-S.; Lees, A. J. *J. Am. Chem. Soc.* **2000**, *122*, 8956. (i) Mosher, P. J.; Yap, G. P. A.; Crutchley, R. J. *Inorg. Chem.* **2001**, *40*, 1189−1195.

10.1021/ic0260466 CCC: $25.00
Published on Web 09/03/2003

reversible redox reaction of the metal center and single light irradiation[5g,i] and MLCT photoisomerization,[5e,i] indicating that the type of attached metal complex controls such functionalities.

We have constructed an azobenzene-conjugated terpyridine transition metal complex system[6] and carried out a systematic study of its trans−cis isomerization and other photochemical and electrochemical behavior, as dependent on metal centers, composed of Ru(II),[6a,c] Rh(III),[6b,c] and Pt(II)[6d] complexes. Ru(II) complexes showed only a 20% trans-to-cis photoisomerization because of the energy transfer from the azobenzene unit to the $Ru(tpy)_2$ units. In contrast, Rh(III) complexes showed complete trans-to-cis photoisomerization, with the behavior being dependent on solvents and counterions, and the generated cis form appears to have a very long lifetime. Pt(II) complexes showed reversible trans−cis isomerization, and photoluminescence switching linked to the trans−cis configuration change was observed. These results indicate that the photoisomerization properties of the azobenzene moiety in the complexes are significantly dependent on the central metals and are perturbed by the complex units with intense MLCT bands in the visible region due to the energy transfer.

In this study, we employed azobenzene-bound terpyridine complexes of the 3d metals, cobalt and iron, and compared them with previously created complexes of 4d metals, rhodium and ruthenium, belonging to the same group, respectively. It is well-known that Co−polypyridine complexes show reversible electrochemical behavior[7] and have no intense MLCT or d−d bands, but very weak bands in the visible region.[7f−h,8] Under the normal synthetic conditions, we can obtain the complexes in which the cobalt center is divalent, but we can easily generate trivalent cobalt complexes by adding an appropriate oxidizing agent or even by air-oxidization[9] because the redox potential of Co(II)/Co(III) is near 0 V versus NHE. It should be mentioned that

Chart 1

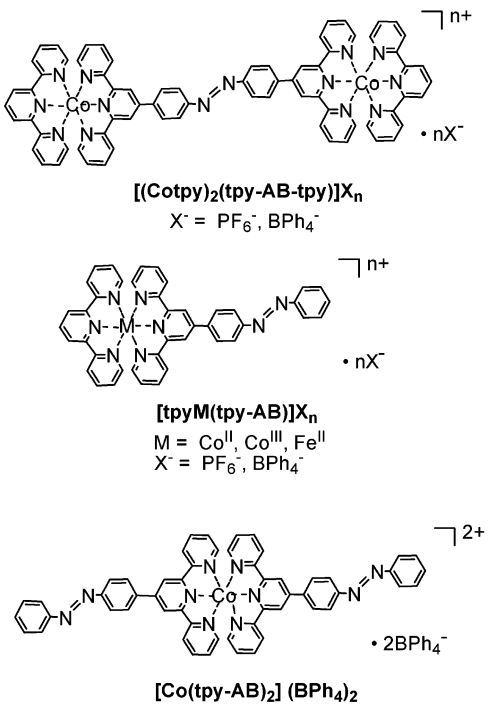

we have found redox-combined single light reversible isomerization for tris(azobenzene-bound bipyridine)cobalt.[5g] There have been many reports of Fe−terpyridine complexes,[10] with recent studies having been focused on the reversible redox properties and spin-crossover behavior. Herein, we present syntheses of new azobenzene-bound Co(II), Co(III), and Fe(II) complexes (Chart 1), and we describe their photochemical and electrochemical properties.

Experimental Section

Materials. 2,2′:6′,2″-Terpyridine (tpy),[11] $CoCl_2$tpy,[12] $FeCl_2$tpy,[13] tpy-AB,[6c] and tpy-AB-tpy[6a] were prepared according to the literature. Ammonium hexafluorophosphate (NH_4PF_6), sodium tetraphenylborate ($NaBPh_4$), $CoCl_2 \cdot 6H_2O$, and $FeCl_2 \cdot 4H_2O$ were purchased from Kanto Chemicals and used as received. For UV−vis spectroscopy, dimethyl sulfoxide, propylene carbonate (Kanto Chemicals, guaranteed grade), and *N*,*N*-dimethylformamide (Dojin, spectroscopic grade) were used as received. Propylene carbonate used for the electrochemical measurements was of HPLC grade. Tetrabutylammonium tetrafluoroborate (lithium-battery grade) for the electrochemical measurements was obtained from Tomiyama Chemicals.

(5) (a) Hayami, S.; Inoue, K.; Osaki, S.; Maeda, Y. *Chem. Lett.* **1998**, 987−988. (b) Yam, V. W.-W.; Lau, V. C.-Y.; Wu, L.-X. *J. Chem. Soc., Dalton. Trans.* **1998**, 1461−1468. (c) Tsuchiya, S. *J. Am. Chem. Soc.* **1999**, *121*, 48−53. (d) Aiello, I.; Ghedini, M.; La Deda, M.; Pucci, D.; Francescangeli, O. *Eur. J. Inorg. Chem.* **1999**, 1367−1372. (e) Kurihara, M.; Matsuda, T.; Hirooka, A.; Yutaka, T.; Nishihara, H. *J. Am. Chem. Soc.* **2000**, *122*, 12373−12374. (f) Nihei, M.; Kurihara, M.; Mizutani, J.; Nishihara, H. *Chem. Lett.* **2001**, 852−853. (g) Kume, S.; Kurihara, M.; Nishihara, H. *J. Chem. Soc., Chem. Commun*. **2001**, 1656−1657. (h) Kurihara, M.; Nishihara, H. *Coord. Chem. Rev.* **2002**, *226*, 125−135. (i) Kurihara, M.; Hirooka, A.; Kume, S.; Sugimoto, M.; Nishihara, H. *J. Am. Chem. Soc.* **2002**, *124*, 8800−8801.

(6) (a) Yutaka, T.; Kurihara, M.; Nishihara, H. *Mol. Cryst. Liq. Cryst*. **2000**, *343*, 511−516. (b) Yutaka, T.; Kurihara, M.; Kubo, K.; Nishihara, H. *Inorg. Chem.* **2000**, *39*, 3438−3439. (c) Yutaka, T.; Mori, I.; Kurihara, M.; Mizutani, J.; Kubo, K.; Furusho, S.; Matsumura, K.; Tamai, N.; Nishihara, H. *Inorg. Chem*. **2001**, *40*, 4986−4995. (d) Yutaka, T.; Mori, I.; Kurihara, M.; Mizutani, J.; Tamai, N.; Kawai, T.; Irie, M.; Nishihara, H. *Inorg. Chem.* **2002**, *41*, 7143−7150.

(7) (a) Rao, J. M.; Hughes, M. C.; Macero, D. J. *Inorg. Chim. Acta* **1976**, *16*, 231−236. (b) Rao, J. M.; Macero, D. J.; Hughes, M. C. *Inorg. Chim. Acta* **1980**, *4*, 221−226. (c) Ruminski, R. R.; Petersen, J. D. *Inorg. Chim. Acta* **1985**, *97*, 129−134. (d) Guadalupe, A. R.; Usifer, D. A.; Potts, K. T.; Hurrell, H. C.; Mogstad, A.-E.; Abruña, H. D. *J. Am. Chem. Soc*. **1988**, *110*, 3462−3466. (e) Ramprasad, D.; Gilicinski, A. G.; Markley, T. J.; Pez, G. P. *Inorg. Chem*. **1994**, *33*, 2841−2847. (f) Storrier, G. D.; Colbran, S. B.; Craig, D. C. *J. Chem. Soc., Dalton Trans*. **1997**, 3011−3028. (g) Storrier, G. D.; Colbran, S. B.; Craig, D. C. *J. Chem. Soc., Dalton Trans*. **1998**, 1351−1363.

(8) Judge, J. S.; Baker, W. A. *Inorg. Chim. Acta* **1967**, *1*, 68−72.

(9) Figgis, B. N.; Kucharski, E. S.; White, A. H. *Aust. J. Chem*. **1983**, *36*, 1563−1571.

(10) (a) Constable, E. C.; Ward, M. D.; Corr, S. *Inorg. Chim. Acta* **1988**, *141*, 201−203. (b) Braterman, P. S.; Song, J.-I.; Peacock, R. D. *Inorg. Chem*. **1992**, *31*, 555−559. (c) Gütlich, P.; Hauser, A.; Spiering, H. *Angew. Chem., Int. Ed. Engl*. **1994**, *33*, 2024−2054. (d) Storrier, G. D.; Colbran, S. B.; Hibbert, D. B. *Inorg. Chim. Acta* **1995**, *239*, 1−4. (e) Hathcock, D. J.; Stone, K.; Madden, J.; Slattery, S. J. *Inorg. Chim. Acta* **1998**, *282*, 131−135. (f) Constable, E. C.; Baum, G.; Bill, E.; Raylene, D.; van Eldik, R.; Fenske, D.; Kaderli, S.; Morris, D.; Neubrand, A.; Neuburger, M.; Smith, D. R.; Wieghardt, K.; Zehnder, M.; Zuberbühler, A. D. *Chem. Eur. J*. **1999**, *5*, 498−508. (g) Kimura, M.; Horai, T.; Muto, T.; Hanabusa, K.; Shirai, H. *Chem. Lett*. **1999**, 1129−1130. (h) Priimov, G. U.; Moore, P.; Maritim, P. K.; Butalanyi, P. K.; Alcock, N. W. *J. Chem. Soc., Dalton Trans*. **2000**, 445−449.

(11) Jameson, D. L.; Guise, L. E. *Tetrahedron Lett.* **1991**, *32*, 1999−2002.

(12) Harris, C. M.; Lockyer, T. N.; Martin, R. L.; Patil, H. R. H.; Sinn, E.; Stewart, I. M. *Aust. J. Chem*. **1969**, *22*, 2105−2116.

(13) Broomhead, J. A.; Dwyer, F. P. *Aust. J. Chem.* **1961**, *14*, 250−252.

Table 1. Crystal Data and Structure Refinement Details for $[Co(tpy\text{-}AB)_2](BPh_4)_2$

empirical formula	$C_{106}H_{84}N_{12}B_2Co$
fw	1606.46
cryst dimens	$0.40 \times 0.30 \times 0.20$ mm^3
cryst syst	monoclinic
a (Å)	22.895(5)
b (Å)	21.1422(11)
c (Å)	18.7864(5)
β (deg)	106.8040(7)
V (Å^3)	8705.1(14)
space group	$C2/c$
Z value	4
D_{calcd}	1.226 g/cm^3
F_{000}	3364.00
residuals, R; R_w	0.097; 0.116

Apparatus. UV−vis, IR, ^{1}H NMR, and ESI mass spectra were recorded with Jasco V-570 and Hewlett-Packard 8453 UV−vis spectrometers, a Jasco FT/IR-62-v spectrometer, JEOL EX270 and Brucker AM 500 spectrometers, and a Micromass LCT (time-of-flight mass spectrometer), respectively. Photoisomerization measurements were carried out under a nitrogen atmosphere using a 500 W super high-pressure mercury lamp USH-500D (USHIO) as an irradiation source. The 366-nm light was isolated with a UV-D35 Toshiba glass filter. The 435-nm light was isolated with a combination of a Y-43 Toshiba glass filter and KL-44 Toshiba interference filter.

Crystal Structure Determination. $[Co(tpy\text{-}AB)_2](BPh_4)_2 \cdot 2CH_3CN$ was crystallized as red-brown blocks by slow diffusion from diethyl ether into an acetonitrile solution. Selected crystallographic data and experimental details are listed in Table 1 (see Supporting Information).

Measurements of Trans−Cis Isomerization and Quantum Yields. A 1-cm light path-length quartz cell was used for the photoisomerization measurements. The sample concentration was approximately 1×10^{-5} M. Sample solution was degassed by N_2 bubbling before photoirradiation and stirred during trans-to-cis and cis-to-trans isomerization. The cis-to-trans thermal isomerization rate was measured by the "kinetic" mode of Hewlett-Packard 8453 UV−vis spectrometers, where the UV−vis spectra were measured continuously with determined intervals at a given constant temperature. Quantum yields of trans-to-cis photoisomerization were measured for each complex using $K_3[Fe(C_2O_4)_3]$ as a chemical actinometer from the absorbance changes within a 10% trans-to-cis structural conversion.

Electrochemical Measurements. A glassy carbon rod (diameter 5 mm; Tokai Carbon GC-20) was embedded in Pyrex glass, and the cross-section was used as a working electrode. Cyclic voltammetry measurements were carried out in a standard one-compartment cell equipped with a platinum-wire counter electrode and a Ag/Ag^+ reference electrode under Ar with a BAS CV-50W voltammetric analyzer.

Femtosecond Transient Absorption Spectra. The arrangement for the femtosecond pump−probe experiment was essentially the same as that reported elsewhere.[14] Briefly, the laser system consisted of a hybridly mode-locked, dispersion-compensated femtosecond dye laser (Coherent, Satori 774) and a dye amplifier (Continuum, RGA 60−10 and PTA 60). The dye laser (gain dye Pyridine 2 and saturable absorber DDI) was pumped with a cw mode-locked Nd:YAG laser (Coherent, Antares 76S). The sample was excited by the second harmonic (360 nm) of the fundamental (center wavelength 720 nm, pulse width ~200 fs fwhm) at a repetition rate of 10 Hz. The residual portion of the fundamental output was focused on a 1-cm H_2O cell to generate a femtosecond supercontinuum probe pulse. The planes of polarization of the pump and probe beams were set to the magic angle (54.7°) to avoid any anisotropic contribution to the transient signal. Both beams were focused on the sample in a 2-mm cuvette at an angle of less than 5°. Transient spectra were obtained by averaging over 200 pulses and analyzed by an intensified multichannel detector (Princeton Instruments, ICCD-576) as a function of the probe-delay time. The spectra were corrected for the intensity variations and time dispersions of the supercontinuum. Rise and decay curves at a fixed wavelength were measured with a photodiode−monochromator (Japan Spectroscopic, CT-10) combination. The sample concentration for transient absorption spectra was kept within a range $1-1.5 \times 10^{-4}$ M. The solution was allowed to flow through a 2-mm flow cell using a magnetically coupled gear pump (Micropump, 040−332) to avoid any possibility of sample damage during the transient absorption measurement.

Syntheses. A General Synthetic Procedure for $[(Cotpy)_2(tpy\text{-}AB\text{-}tpy)]X_4$ and $[tpyCo^{II}(tpy\text{-}AB)]X_2$ ($X^- = PF_6^-$ or BPh_4^-). A mixture of $CoCl_2tpy$ (0.069 g, 0.15 mmol) and tpy-AB-tpy (0.050 g, 0.077 mmol) in ethylene glycol (5 mL) was heated at reflux for 1 h. After the mixture was cooled to room temperature and filtered off, excess NH_4PF_6 or $NaBPh_4$ in water (30 mL) was added to the filtrate. The precipitate formed was centrifuged and filtered, and then recrystallized from acetonitrile−ether to yield red powders. The mononuclear complexes, $[tpyCo^{II}(tpy\text{-}AB)]X_2$'s, were prepared by the similar method of $(Cotpy)_2(tpy\text{-}AB\text{-}tpy)\cdot 4PF_6$ except for using tpy-AB instead of tpy-AB-tpy.

$[(Cotpy)_2(tpy\text{-}AB\text{-}tpy)](PF_6)_4$. Yield 80%. Anal. Calcd for $C_{72}H_{50}N_{14}Co_2F_{24}P_4$: C, 47.78; H, 2.79; N, 10.84. Found: C, 47.91; H, 3.00; N, 10.56. ESI MS m/z 759.13 ($[(Cotpy)_2(tpy\text{-}AB\text{-}tpy)\cdot 2PF_6]^{2+}$ requires 759.11), 457.76 ($[(Cotpy)_2(tpy\text{-}AB\text{-}tpy)\cdot 1PF_6]^{3+}$ requires 457.75), 307.08 ($[(Cotpy)_2(tpy\text{-}AB\text{-}tpy)]^{4+}$ requires 307.07).

$[(Cotpy)_2(tpy\text{-}AB\text{-}tpy)](BPh_4)_4$. Yield 40%. The sample for elemental analysis was purified from DMF−ether. Anal. Calcd for $C_{168}H_{130}N_{14}B_4Co_2\cdot 3DMF\cdot 2H_2O$: C, 76.99; H, 5.66; N, 8.62. Found: C, 76.70; H, 5.36; N, 8.51. ESI MS m/z 933.84 ($[(Cotpy)_2(tpy\text{-}AB\text{-}tpy)\cdot 2BPh_4]^{2+}$ requires 933.82), 516.15 ($[(Cotpy)_2(tpy\text{-}AB\text{-}tpy)\cdot 1BPh_4]^{3+}$ requires 516.16), 307.08 ($[(Cotpy)_2(tpy\text{-}AB\text{-}tpy)]^{4+}$ requires 307.07).

$[tpyCo^{II}(tpy\text{-}AB)](PF_6)_2$. Yield 64%. Anal. Calcd for $C_{42}H_{30}N_8CoF_{24}P_2$: C, 50.67; H, 3.04; N, 11.25. Found: C, 50.75; H, 3.15; N, 11.10. ESI MS m/z 850.13 ($[tpyCo^{II}(tpy\text{-}AB)\cdot 1PF_6]^+$ requires 850.16), 352.60 $[tpyCo^{II}(tpy\text{-}AB)]^{2+}$ requires 352.60).

$[tpyCo^{II}(tpy\text{-}AB)](BPh_4)_2$. Yield 59%. Anal. Calcd for $C_{90}H_{70}N_8B_2Co\cdot H_2O$: C, 79.36; H, 5.33; N, 8.23. Found: C, 79.12; H, 5.29; N, 8.19. ESI MS m/z 352.61 ($[tpyCo^{II}(tpy\text{-}AB)]^{2+}$ requires 352.60).

$[tpyCo^{III}(tpy\text{-}AB)](PF_6)_3$. $tpyCo^{II}(tpy\text{-}AB)\cdot 2PF_6$ (0.051 g, 0.051 mmol) was dissolved in hot methanol (150 mL), and the solution was added dropwise into the methanolic solution (5 mL) of $AgCF_3SO_3$ (0.080 g, 0.31 mmol). The mixture was heated at reflux overnight and filtered through a Celite layer. After excess NH_4PF_6 was added, the red solution was evaporated until a red precipitate appeared. The red precipitate was filtered and recrystallized from acetonitrile−ether. Yield 0.041 g (70%).

Anal. Calcd for $C_{42}H_{30}N_8CoF_{18}P_3$: C, 44.23; H, 2.65; N, 9.82. Found: C, 44.17; H, 2.83; N, 9.77. ^{1}H NMR (CD_3CN): δ 9.35 (d, 2H, $J = 5.5$ Hz), 9.12 (t, 2H, $J = 7.5$ Hz), 9.03 (d, 2H, $J = 5.5$ Hz), 8.75 (t, 2H, $J = 8.4$ Hz), 8.60 (t, 2H, $J = 8.4$ Hz), 8.53 (t, 2H, $J = 7.6$ Hz), 8.37 (m, 2H), 8.31−8.23 (m, 4H), 8.08−8.06 (m, 2H), 7.70−7.67 (m, 3H), 7.50−7.39 (m, 6H), 7.27 (d, 2H, $J =$ 5.0 Hz). ESI MS m/z 995.10 ($[tpyCo^{III}(tpy\text{-}AB)\cdot 2PF_6]^+$ requires

(14) (a) Tamai, N.; Masuhara, H. *Chem. Phys. Lett.* **1992**, *191*, 189−194. (b) Mitra, S.; Tamai, N. *Chem. Phys. Lett.* **1998**, *282*, 391−397.

995.12), 425.08 ($[tpyCo^{III}(tpy\text{-}AB)\cdot 1PF_6]^{2+}$ requires 425.08), 235.04 ($[tpyCo^{III}(tpy\text{-}AB)]^{3+}$ requires 235.07).

$[Co(tpy\text{-}AB)_2](BPh_4)_2$. A mixture of $CoCl_2\cdot 6H_2O$ (0.028 g, 0.12 mmol) and tpy-AB (0.099 g, 0.24 mmol) in MeOH (7 mL) was heated at reflux for 30 min. After the solution was cooled to room temperature and filtered, excess $NaBPh_4$ in water (30 mL) was added. The precipitate was filtered and recrystallized from acetonitrile−ether to yield red powders. Yield 0.097 g (53%).

Anal. Calcd for $C_{102}H_{78}N_{10}B_2Co$: C, 80.37; H, 5.16; N, 9.19. Found: C, 80.10; H, 5.16; N, 9.19. ESI MS *m*/*z* 442.63 ($[Co(tpy\text{-}AB)_2]^{2+}$ requires 442.63).

$Co^{III}(tpy)_2\cdot 3PF_6$. This complex was prepared from $Co^{II}(tpy)_2\cdot 2PF_6$ by a method similar to that for $tpyCo^{III}(tpy\text{-}AB)\cdot 3PF_6$. Yield 60%. Anal. Calcd for $C_{30}H_{22}N_6CoF_{18}P_3$: C, 37.52; H, 2.31; N, 8.75. Found: C, 37.52; H, 2.43; N, 8.48. ^{1}H NMR (CD_3CN): δ 9.10 (dd, 1H, J = 9.1, 6.4 Hz), 9.00 (dd, 2H, J = 8.1, 2.4 Hz), 8.61 (dd, 2H, J = 8.0, 1.4 Hz), 8.23 (td, 2H, J = 7.8, 1.4 Hz), 7.44 (ddd, 2H, J = 7.7, 6.2, 1.6 Hz), 7.24 (dd, 2H, J = 6.2, 1.1 Hz).

A General Synthetic Procedure for $[tpyFe(tpy\text{-}AB)]X_2$ (X^- = PF_6^- or BPh_4^-). A mixture of $FeCl_2tpy$ (0.087 g, 0.24 mmol) and tpy-AB (0.099 g, 0.24 mmol) in ethylene glycol (5 mL) was heated at reflux for 1 h. After the solution was cooled to room temperature and filtered, excess NH_4PF_6 or $NaBPh_4$ in water (30 mL) was added. The precipitate was filtered and recrystallized from acetonitrile−ether to yield violet powders.

$[tpyFe(tpy\text{-}AB)](PF_6)_2$. Yield 75%. Anal. Calcd for $C_{42}H_{30}N_8FeF_{12}P_2$: C, 50.83; H, 3.05; N, 11.29. Found: C, 50.54; H, 3.25; N, 11.27. ^{1}H NMR (CD_3CN): δ 9.24 (d, 2H, J = 7.0 Hz), 8.93 (t, 1H, J = 7.0 Hz), 8.71−8.61 (m, 4H), 8.53−8.43 (m, 4H), 8.32 (dd, 2H, J = 8.6, 2.1 Hz), 8.05 (m, 2H), 7.96−7.85 (m, 4H), 7.68−7.62 (m, 3H), 7.21 (t, 2H, J = 5.6 Hz), 7.13−7.04 (m, 6H). ESI MS *m*/*z* 351.10 ($[tpyFe(tpy\text{-}AB)]^{2+}$ requires 351.10).

$[tpyFe(tpy\text{-}AB)](BPh_4)_2$. Yield 89%. Anal. Calcd for $C_{90}H_{70}N_8FeB_2\cdot H_2O$: C, 79.54; H, 5.34; N, 8.25. Found: C, 79.71; H, 5.46; N, 8.16. ^{1}H NMR (CD_3CN): δ 9.03 (d, 2H, J = 7.0 Hz), 8.66 (t, 4H, J = 7.6 Hz), 8.49−8.38 (m, 3H), 8.30 (d, 2H, J = 8.6 Hz), 8.23 (t, 4H, J = 7.0 Hz), 8.12 (d, 2H, J = 8.2 Hz), 7.86 (d, 2H, J = 8.2 Hz), 7.67 (td, 2H, J = 7.4, 1.0 Hz), 7.46 (d, 2H, J = 7.0 Hz), 7.09−7.03 (m, 16H), 6.98 (d, 2H, J = 6.0 Hz), 6.90−6.82 (m, 5H), 6.78 (t, 16H, J = 7.3 Hz), 6.62 (t, 8H, J = 7.3 Hz). ESI MS *m*/*z* 1021.39 ($[tpyFe(tpy\text{-}AB)\cdot 1BPh_4]^+$ requires 1021.39), 351.10 ($[tpyFe(tpy\text{-}AB)]^{2+}$ requires 351.10).

Results and Discussion

Syntheses and Characterization. Azobenzene-conjugated mono- and dinuclear Co complexes were obtained by the reaction of $CoCl_2tpy$ with the corresponding azobenzene-containing terpyridine ligand. Anions PF_6^- and BPh_4^- were selected as counterions because the photoisomerization behavior was much affected by the counterions in a previous study on Rh complexes,[6c] and the most remarkable difference was observed in the complexes using these two counterions. The Co complex salts of both counterions were soluble in acetonitrile (MeCN), *N*,*N*-dimethylformamide (DMF), dimethyl sulfoxide (DMSO), propylene carbonate (PC), etc., but the solubility was quite lower than that of the corresponding Rh and Ru complexes.[6] The Co^{III} complexes were easily prepared by the oxidation with Ag^+.[5g] The solubility of the PF_6^- salt of the Co^{III} complex was much less than that of the Co^{II} complex. $[Co(tpy\text{-}AB)_2](BPh_4)_2\cdot 2CH_3CN$ was obtained in the recrystallization process of $[tpyCo^{II}(tpy\text{-}AB)](BPh_4)_2$ by the vapor diffusion of diethyl ether to the highly concentrated acetonitrile solution because the ligand-exchange from tpy to tpy-AB easily occurred. This complex was also obtained according to the general synthetic method of CoL_2 (L = tridentate ligands), and its molecular structure was determined by a single-crystal X-ray diffraction analysis. An ORTEP diagram with representative bond lengths and angles is shown in Figure 1, indicating the involvement of two normal trans-azobenzene structures in the molecule.

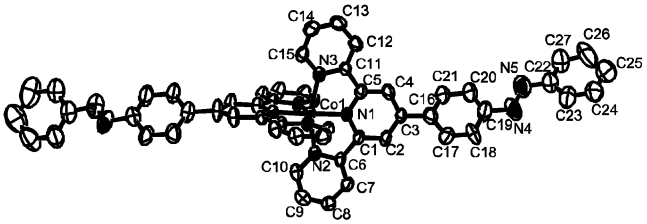

Figure 1. ORTEP view of $[Co(tpy\text{-}AB)_2](BPh_4)_2\cdot 2CH_3CN$ with 50% probability. H atoms, BPh_4^- ions, and acetonitrile are omitted for clarity. Selected bond lengths (Å), bond angles (deg), and torsion angles (deg) are as follows: Co(1)−N(1) 1.878(4), Co(1)−N(2) 2.071(5), N(4)−N(5) 1.284(11), N(1)−Co(1)−N(2) 80.2(2), N(2)−Co(1)−N(3) 160.3, N(5)−N(4)−C(19) 113.3(10), N(5)−N(4)−C(19)−C(20) 7.2(20), N(4)−N(5)−C(22)−C(27) 163.8(13), C(4)−C(3)−C(16)−C(17) 134.2.

The Fe mononuclear complexes were prepared from $FeCl_2$-tpy by a two-step reaction similar to that of the Co complexes. All the Co and Fe complexes were characterized by UV−vis, ^{1}H NMR (except for Co^{II} complexes), ESI MS spectra, and elemental analysis.

UV−vis absorption spectra of $tpyCo^{II}(tpy\text{-}AB)\cdot 2PF_6$, tpy-AB, and $Co^{II}(tpy)_2\cdot 2PF_6$ are shown in Figure 2A, inset. The spectrum of $tpyCo^{II}(tpy\text{-}AB)\cdot 2PF_6$ can be interpreted by the superposition of tpy-AB and $Co^{II}(tpy)_2\cdot 2PF_6$, exhibiting an intense peak at 320 nm ascribable to a ligand-centered (LC) band,[7] and three weak peaks at 446, 504, and 545 nm assignable to d−d transition or MLCT of the cobalt complex moiety.[8] A similar tendency is observed for $(Cotpy)_2(tpy\text{-}AB\text{-}tpy)\cdot 4PF_6$, as shown in Figure 2B, inset. UV−vis absorption spectra of Co^{III} complexes in 1,2-dichloroethane are shown in Figure 3, inset. In the spectrum of $Co^{III}(tpy)_2\cdot 3PF_6$, except for a LC band at 320 nm, there were no intense bands observed in the visible region. It can be seen that the azo $\pi-\pi^*$ band of $tpyCo^{III}(tpy\text{-}AB)\cdot 3PF_6$ is more broadened and red-shifted than that of $tpyCo^{II}(tpy\text{-}AB)\cdot 2PF_6$. The broad band at 400−500 nm is smaller than the spectrum of $tpyCo^{II}(tpy\text{-}AB)\cdot 2PF_6$; this broad band decreases in size, and the overlapped band of azo $\pi-\pi^*$ and LC is red-shifted by 70 nm.

A UV−vis absorption spectrum of $tpyFe(tpy\text{-}AB)\cdot 2PF_6$ is shown in Figure 4 inset. An intense MLCT band appears at 580 nm, which is more intense and red-shifted than that of $Fe(tpy)_2\cdot 2PF_6$, suggesting the presence of significant π-conjugation between the azobenzene unit and the $Fe(tpy)_2$ unit.

Photochemical and Thermal Isomerization Behavior of the Co^{II} Complexes. UV−vis spectral changes of $tpyCo^{II}(tpy\text{-}AB)\cdot 2PF_6$ and $(Cotpy)_2(tpy\text{-}AB\text{-}tpy)\cdot 4PF_6$ in propylene carbonate (PC) upon irradiation with 366-nm light are shown in Figure 2A,B, respectively. Mono- and dinuclear BPh_4^-

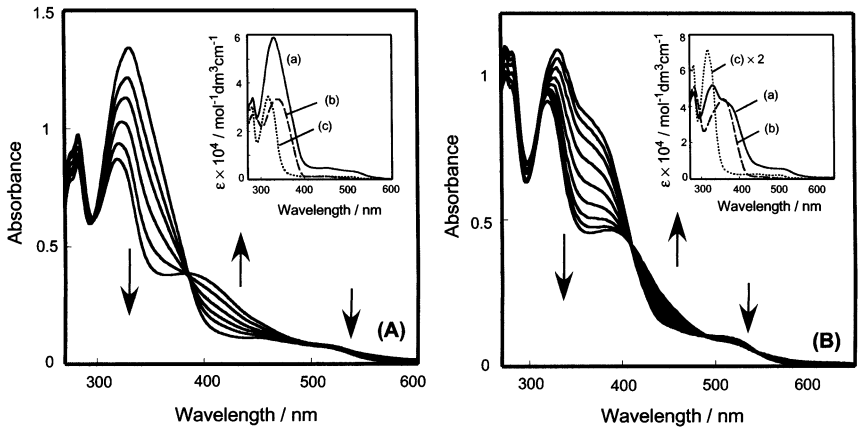

Figure 2. (A) UV−vis spectral change of tpyCo^{II}(tpy-AB)·2BPh$_4$ (2.2×10^{-5} M) in PC upon irradiation at 366 nm for 40 min. Inset: Spectra of tpyCo^{II}(tpy-AB)·2PF$_6$ (a), tpy-AB (b), and Co^{II}(tpy)$_2$·2PF$_6$ (c). (B) UV−vis spectral change of (Cotpy)$_2$(tpy-AB-tpy)·4BPh$_4$ (1.8×10^{-5} M) in PC upon irradiation at 366 nm for 1 h. Inset: Spectra of (Cotpy)$_2$(tpy-AB-tpy)·4PF$_6$ (a), tpy-AB-tpy (b), and Co^{II}(tpy)$_2$·2PF$_6$ (c).

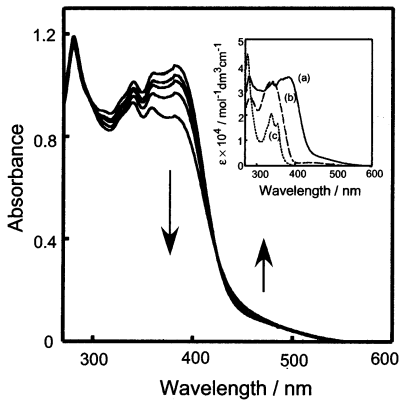

Figure 3. UV−vis spectral change of tpyCo^{III}(tpy-AB)·3PF$_6$ (2.7×10^{-5} M) in 1,2-dichloroethane upon irradiation at 366 nm for 25 min. Inset: Spectra of tpyCo^{III}(tpy-AB)·3PF$_6$ (a), tpy-AB (b), and Co^{III}(tpy)$_2$·3PF$_6$ (c).

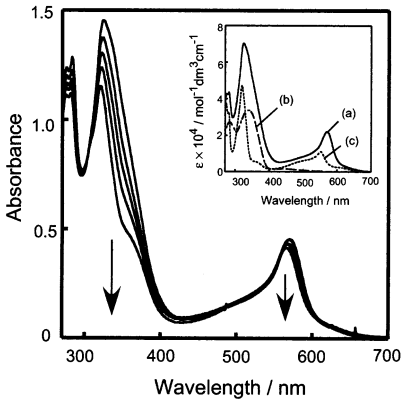

Figure 4. UV−vis spectral change of tpyFe(tpy-AB)·2PF$_6$ (2.0×10^{-5} M) in acetonitrile upon irradiation at 366 nm for 20 min. Inset: Spectra of tpyFe(tpy-AB)·2PF$_6$ (a), tpy-AB (b), and Fe(tpy)$_2$·2PF$_6$ (c).

salts exhibited similar spectral changes with PF_6^- salts upon photoirradiation. The absorbance of the azo $\pi-\pi^*$ transition band decreases, and that of the azo n$-\pi^*$ transition band increases with three isosbestic points. These results indicate that trans-to-cis photoisomerization behavior of the mononuclear and dinuclear Co complexes is observed. In the cis form, an intense band appears in the visible region as with Rh complexes,[6] assignable to the azo n$-\pi^*$ band. But this band is much more intense than that of organic azobenzenes. Rau has reported that a low-lying azo n$-\pi^*$ state can interact with other molecular states such as the neighboring azo $\pi-\pi^*$ state.[15] In the complexes in this study, the terpyridine $\pi-\pi^*$ band is superposed with the broad azo $\pi-\pi^*$ band. Accordingly, the appearance of these intense bands indicates that the azo n$-\pi^*$ band overlaps the intensity of the low-lying, neighboring state, azo $\pi-\pi^*$, and terpyridine $\pi-\pi^*$ states.

Significant spectral changes due to trans-to-cis photoisomerization were observed in DMSO and PC, although the photostationary state was found to be more lopsided to the trans form in MeCN than in other solvents. On the other hand, spectral changes by photoirradiation in DMF were extremely fast and complicated, probably because the dissociation of tpy-AB or tpy-AB-tpy ligand occurred and the free ligand exhibited trans-to-cis isomerization. This is supported by the fact that recrystallization of tpyCo^{II}(tpy-AB) in DMF afforded Co(tpy-AB)$_2^{2+}$ by the facile ligand exchange reaction as described. Co(II) complexes are known to be labile to ligand exchange, but we selected the solvents to afford simple spectral change without dissociation and ligand exchange, for the photoreaction of the complexes. The photoproducts could be isolated by precipitation from PC solution by adding 1,4-dioxane and characterized by IR spectroscopy for (Cotpy)$_2$(tpy-AB-tpy)·4PF$_6$. The peak ascribed to N═N stretching of the cis form appeared at 1534 cm^{-1}. Trans-to-cis photoisomerization process was also monitored by the transient absorption spectroscopy (vide infra). The quantum yields ($\Phi_{t\rightarrow c}$) of Co complexes for trans-to-cis photoisomerization are listed in Table 2. There are three characteristic features, different from those of Rh complexes:[6c] (1) $\Phi_{t\rightarrow c}$ of Co complexes is much smaller, (2) solvent effect is observed and $\Phi_{t\rightarrow c}$ increases in the order of PC > DMSO, which is reverse, compared with those of the Rh complexes, and (3) counterion effect is less evident. All the $\Phi_{t\rightarrow c}$ values in DMSO and PC are within a small range from 3×10^{-4} to 8×10^{-4}, and accordingly, solvent and counterion have less influence on the trans-to-cis photo-

(15) Rau, H. *Angew. Chem., Int. Ed. Engl.* **1973**, *12*, 224−235.

Table 2. Trans-to-Cis Photoisomerization Quantum Yields ($\Phi_{t\rightarrow c}$) of the Co Complexes

			$10^4\ \Phi_{t\rightarrow c}$			
solvent	dielectric constant,[a] ϵ	viscosity[a] (η/mPa s)	$tpyCo^{II}$-(tpy-AB)·$2PF_6$	$tpyCo^{II}$-(tpy-AB)·$2BPh_4$	$(Cotpy)_2$-(tpy-AB-tpy)·$4PF_6$	$(Cotpy)_2$-(tpy-AB-tpy)·$4BPh_4$
MeCN	36.6	0.369	<1	<1	<1	<1
DMSO	47.2	1.99	3.3	4.3	3.9	5.6
PC	68.8	2.53	7.0	6.2	6.5	8.5

[a] Lide, D. R. *CRC Handbook of Chemistry and Physics*, 79th ed.; CRC Press, Boca Raton, FL.

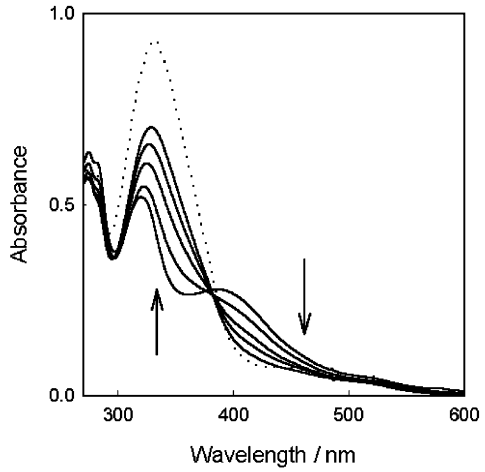

Figure 5. UV−vis absorption spectral change of $tpyCo^{II}$(tpy-AB)·$2BPh_4$ in PC (1.5×10^{-5} M) heated at 90 °C for 12 h. Dotted line indicates the pure trans form.

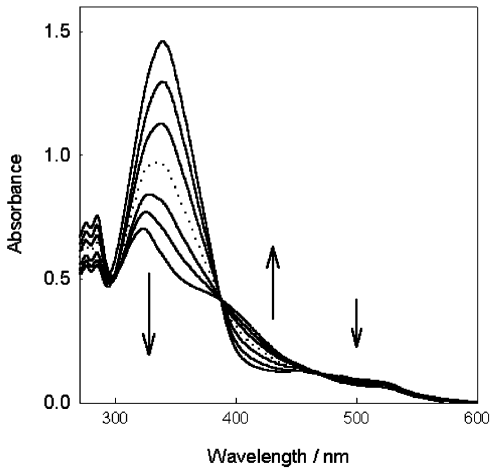

Figure 6. UV−vis spectral change of $[Co(tpy\text{-}AB)_2](BPh_4)_2$ (1.5×10^{-5} M) in PC upon irradiation at 366 nm for 48 min. Dotted line corresponds to the half point, achieved by irradiation at 435 nm for 30 min.

isomerization behavior for the Co complexes than for the Rh complexes. This should be because the Rh complex cation is trivalent, having more charge, and more counterions.

UV−vis spectral change of $tpyCo^{II}$(tpy-AB)·$2BPh_4$ in PC by heating at 90 °C is shown in Figure 5. The trans form was recovered in an approximately 60% yield. $(Cotpy)_2$-(tpy-AB-tpy)·$4BPh_4$ showed the same behavior as $tpyCo^{II}$-(tpy-AB)·$2BPh_4$ under similar conditions. Thermal isomerization rates for $tpyCo^{II}$(tpy-AB)·$2BPh_4$ and $(Cotpy)_2$-(tpy-AB-tpy)·$4BPh_4$, in PC at 90 °C were 1.5×10^{-4} and 2.4×10^{-5}, respectively. Compared with the isomerization rate of ligands (1.5×10^{-3}, for tpy-AB in PC at 90 °C), the isomerization rates of Co complexes are smaller. Although the BPh_4^- salts of the Co complexes exhibit thermal cis-to-trans isomerization in PC, no significant UV−vis spectral change was observed in DMSO by heating at 90 °C. As for the PF_6^- salts, cis-to-trans isomerization behavior was not observed in any solvents even at high temperature. Accordingly, it is suggested that the thermal cis-to-trans isomerization is dependent on the counterions, and the tendency is similar with that of Rh complexes.[6c]

Photochemical cis-to-trans photoisomerization by irradiation with 435-nm light was observed for the mono- and dinuclear Co^{II} complexes in PC, in which the trans form was recovered in a yield of about 60%, whereas no isomerization was observed in DMSO, similar to the results of thermal isomerization already noted. There is no counterion effect on the cis-to-trans photoisomerization. As a conclusion, as for the Co^{II} complexes, the cis form is long-lived in DMSO, and the reversible trans−cis isomerization is observed in PC. As the reason for the incomplete cis-to-trans isomerization already mentioned, partial photodegradation of the compounds cannot be neglected.

Figure 6 shows the UV−vis absorption spectral change of $[Co(tpy\text{-}AB)_2](BPh_4)_2$ upon irradiation with 366-nm light. Apparently, this spectral change is similar to that of $tpyCo^{II}$-(tpy-AB)·$2BPh_4$, although a two-step photoreaction is observed. Half of the change occurred very slowly, taking 30 min, and the latter half occurred at a faster rate, taking 18 min. There are two isosbestic points observed at 366 nm, and the second, at 368 nm. Cis-to-trans photoisomerization by irradiation with 435-nm light occurred, but the spectral change stopped at the half point of the full recovery. These phenomena suggest that two azo groups isomerize in turn, not at the same time.

Photochemical Behavior of the Co^{III} Complex. The UV−vis spectral change of $tpyCo^{III}$(tpy-AB)·$3PF_6$ in 1,2-dichloroethane upon irradiation with 366-nm light is shown in Figure 3. Although the spectral change is not as significant as that of the Rh and Co^{II} complexes, the absorbance of the azo $\pi-\pi^*$ transition band decreased and that of the azo $n-\pi^*$ transition band increased, suggesting that a trans-to-cis photoisomerization also occurs in the Co^{III} complex. Characterization of the photoproduct was difficult because of its low yield and low solubility. The difference in the trans-to-cis photoisomerization yield between Co^{II} and Co^{III} has been also observed for azobenzene-bound tris(bipyridine)cobalt complexes.[5g] It should be noted that the photoreaction of $tpyCo^{III}$(tpy-AB)·$3PF_6$ in PC and in DMSO, which has a higher donor number[16] than 1,2-dichloroethane, causes

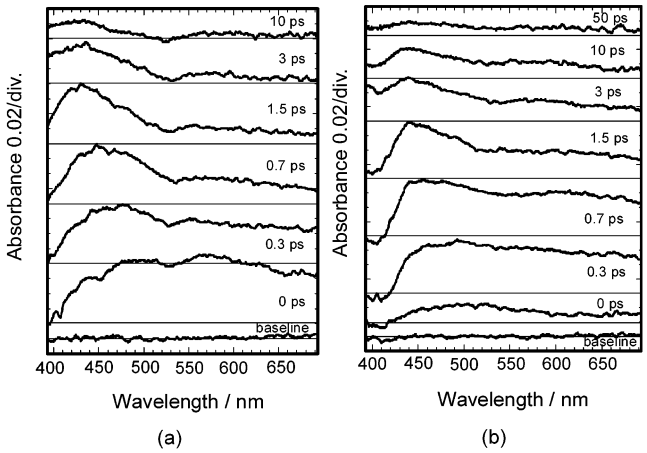

Figure 7. Time-resolved transient absorption spectra of tpyCo^{II}(tpy-AB)·2PF_6 in acetonitrile (a) and tpyCo^{III}(tpy-AB)·3PF_6 (b) in 1,2-dichloroethane upon irradiation at 360 nm.

the reduction to a Co^{II} complex. Trans-to-cis photoisomerization behavior in 1,2-dichloroethane was analyzed by transient absorption spectroscopy (vide infra). In contrast, a cis-to-trans isomerization was not observed by either photoirradiation with visible light or heat. Accordingly, these results suggested that the lifetime of the cis form of the Co^{III} complex is fairly long.

According to these results, Co^{II} and Co^{III} complexes exhibit different photochemical behavior, suggesting that trans−cis isomerization behavior is dependent on both the identity of the metal center and the oxidation state.

Trans-to-Cis Photoisomerization Behavior of the Fe Complexes. The UV−vis spectral change of tpyFe(tpy-AB)·2PF_6 upon irradiation with 366-nm light is shown in Figure 4. Such a slight spectral change upon irradiation is similar to that of the Ru complexes.[6c] The ^{1}H NMR signals in CD_3-CN suggest that the slight spectral change corresponds to the trans-to-cis photoisomerization. In the photostationary state, the ratio of the cis form to the trans form is estimated to be 0.15. The trans-to-cis photoisomerization occurred in acetonitrile and PC but did not occur in DMSO. Instead of photoisomerization, ligand exchange occurred in DMF, which is similar with Co^{II} complexes. It is indicated that there is the dependence of solvent on trans-to-cis photoisomerization. On the other hand, there was no counterion effect; the BPh_4^- salt exhibited the similar behavior to the PF_6^- salt. Cis-to-trans isomerization was observed by both irradiation with 435-nm light and heat, although both processes were very slow (4 days at room temperature).

Transient Absorption Spectra of the Co^{II}, Co^{III}, and Fe^{II} Complexes. Femtosecond transient absorption spectra of tpyCo^{II}(tpy-AB)·2PF_6 and tpyCo^{III}(tpy-AB)·3PF_6 (Figure 7) were measured for direct observation of the photoisomerization reaction of the complex. For the Co^{II} and Co^{III} complexes, the broad $S_n \leftarrow S_2$ ($\pi-\pi^*$) absorption band around 550 nm was observed first, after which the $S_n \leftarrow S_1$ ($n-\pi^*$) absorption band around 450 nm was observed. The lifetime values of the S_2 state are 260 and 230 fs, and those of the S_1 state are 8 and 12 ps for tpyCo^{II}(tpy-AB)·2PF_6 and tpyCo^{III}(tpy-AB)·3PF_6, respectively. These results are similar to those for the Rh complexes and organic azobenzenes which exhibit significant trans-to-cis photoisomerization behavior. The lifetime of the S_1 state, where trans-to-cis photoisomerization is known to occur even in the direct excitation to the S_2 state, is longer than that of the Rh complexes.[6c] This phenomenon may be related to the lower trans-to-cis
photoisomerization quantum yields of the Co^{II} complexes than of the Rh complexes.[6c] As for the Fe complex, very fast bleaching of the Fe MLCT band was observed at 570 nm (Figure 8a). The rise time of the Fe MLCT band of tpyFe(tpy-AB)·2PF_6 is 270 fs (Figure 8b), indicating that the ultrafast energy transfer from the azobenzene unit to the Fe(tpy)$_2$ unit depresses trans-to-cis photoisomerization. The possibility of electron transfer is negligible because the peaks due to the cation radical of azobenzene unit or the anion radical of Fe(tpy)$_2$ unit are not apparently observed in this range.

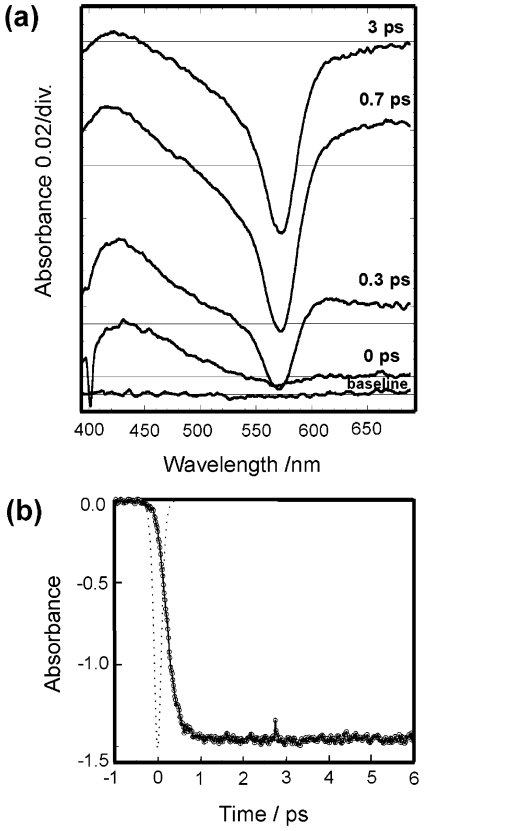

Figure 8. Time-resolved transient absorption spectra (a) and time dependence of absorption spectra at 570 nm (b) of tpyFe(tpy-AB)·2PF_6 in acetonitrile upon irradiation at 360 nm.

In conclusion, the Co complexes, for which the redox reaction is reversible and different from that of the Rh complexes, showed that photoisomerization behavior of the complexes is dependent on the oxidation state of the metal

(16) (a) Gutmann, V. *Coord. Chem. Rev.* **1976**, *18*, 225−255. (b) Gutmann, V. *The Donor−Acceptor Approach to Molecular Interactions*; Plenum: New York, 1980. (c) Donor number (DN) is the absolute value of the heat of mixing of a solution of $SbCl_5$ in 1,2-dichloroethane with another solvent, so DN ≡ 0 for 1,2-dichloroethane, and the value increases with the heat of mixing.

centers. Similar to the Ru complexes,[6c] the Fe^{II} complex shows depressed photoisomerization due to the occurrence of energy transfer.

Acknowledgment. This work was supported by grants-in-aid for scientific research (13022212, 14050032, and 14204066) and a grant-in-aid for The 21st Century COE Program for Frontiers in Fundamental Chemistry from the Ministry of Education, Science, Sports, and Culture, Japan, and the Hayashi Memorial Foundation for Female Natural Scientists.

Supporting Information Available: Details of crystal structure determination and X-ray crystallographic files in CIF format. This material is available free of charge via the Internet at http://pubs.acs.org.

IC0260466